Journal of Catalysis 266 (2009) 250–257

Contents lists available at ScienceDirect

Journal of Catalysis

journal homepage: www.elsevier.com/locate/jcat

Solvated gold atoms in the preparation of efficient supported catalysts: Correlation between morphological features and catalytic activity in the hydrosilylation of 1-hexyne

Laura Antonella Aronica [a], Eleonora Schiavi [a], Claudio Evangelisti [a], Anna Maria Caporusso [a,*], Piero Salvadori [a], Giovanni Vitulli [b], Luca Bertinetti [c], Gianmario Martra [c]

[a] Dipartimento di Chimica e Chimica Industriale, Università di Pisa, Via Risorgimento 35, 56126 Pisa, Italy
[b] Advanced Catalyst s.r.l., Via Risorgimento 35, 56126 Pisa, Italy
[c] Dipartimento di Chimica IFM and NIS Centre of Excellence, Università di Torino, Via P. Giuria 7, 10125 Torino, Italy

ARTICLE INFO

Article history:
Received 23 April 2009
Revised 12 June 2009
Accepted 12 June 2009
Available online 14 July 2009

Keywords:
Gold nanoparticles
Supported catalyst
Metal Vapour Synthesis
Hydrosilylation
HRTEM

ABSTRACT

In the last 20 years, nanostructured gold species have received increasing attention due to their activity in many reactions such as selective oxidations and reductions of fine organic chemicals, both in gas phase and in liquid phase. Here, we report that gold nanoparticles prepared from Au/CH_3COCH_3 solution (obtained from gold vapours and acetone by the Metal Vapour Synthesis technique) can be directly deposited on a wide series of different supports (C, Al_2O_3, Fe_2O_3, CeO_2, TiO_2 and ZrO_2) with their small dimensions being maintained. The supported gold nanoclusters thus obtained are effective catalysts for the hydrosilylation of acetylenic compounds. The catalytic performance of Au is defined by two major factors: particle size and choice of support. For instance, the results obtained from the reaction of 1-hexyne with triethylsilane in the presence of Au/γ-Al_2O_3 (0.05 mol%) demonstrate the high selectivity and the excellent specific activities typical of these gold catalysts.

1. Introduction

Gold is a metal that has fascinated mankind since it was first discovered. Its ductility and its ability to preserve colour and brilliance when exposed to the atmosphere led it to be considered the most noble of metals and used as a base material for many beautiful historical artefacts and works of art. While the golden metal fascinated ancient alchemists, modern chemists considered it too noble to be catalytically active until the last two decades. The discoveries made contemporaneously by Haruta [1] and Hutchings [2] demonstrated that gold, when sub-divided to the nanoscale, could be not only a good catalyst, but even the best catalyst for CO oxidation and ethyne chlorination. In particular, Haruta pointed out that the catalytic activity of gold nanoparticles in the low temperature CO oxidation was markedly enhanced when the particles were less than 6 nm in diameter. Not long after these two discoveries, the interest in gold as a homogeneous and heterogeneous catalyst expanded as demonstrated by several recent reviews [3–9]. Today the "yellow metal" is considered the catalyst of choice for many reactions such as the direct formation of hydrogen peroxide from H_2 and O_2 [10], the hydrogenation of N–O bonds [11], the selective oxidation of hydrocarbons [12–15] (propene and styrene epoxidation, the conversion of cyclohexane to cyclohexanol and cyclohexanone, the oxidation of alcohols to aldehydes and ketones, and of sugars and polyols to acids) and the addition of nucleophiles to C–C multiple bonds. Indeed the ability of gold to coordinate with triple bonds has no parallel with other transition metals. Upon coordination and formation of the corresponding adduct, the alkyne becomes activated and more reactive towards nucleophiles such as alcohols [16], water [17], amines [18] and hydrosilanes.

In the field of hydrosilylation reactions, gold was ignored until 2000 when Hosomi and co-workers [19] described the first example of silane addition to aldehydes using a catalytic amount of AuCl(PPh_3). Their work stimulated other research groups [20–25] that investigated gold-catalyzed hydrosilylations of carbonyl and olefin substrates. Recently, we published [26] the regioselective hydrosilylation of 1-hexyne activated by gold nanoparticles supported on carbon and γ-Al_2O_3. We compared the catalytic performance of gold species with the performance of platinum-based catalysts and observed an opposite affinity between the two metals and the silanes. Indeed, a gold catalyst was required in the reactions performed with Me_2PhSiH or Et_3SiH, while a platinum species had to be used in the presence of chlorosilanes. Both platinum- and gold-supported nanoparticles were generated using the Metal Vapour Synthesis technique [27] (MVS), a versatile method that can be employed for the preparation of colloidal solutions of metal nanoclusters, which can be directly deposited

* Corresponding author. Fax: +39 0502219260.
E-mail address: capored@dcci.unipi.it (A.M. Caporusso).

0021-9517/$ - see front matter © 2009 Elsevier Inc. All rights reserved.
doi:10.1016/j.jcat.2009.06.012

on organic or inorganic matrices with a chosen metal loading and without any further activation process. In the case of gold-supported catalysts, the dimensions of the particles are quite important since it is now well established that the catalytic activity of Au depends on a large extent on the size of the nanoparticles [1,3–9], but other effects such as the nature of the support material, the Au/support interface, the particle shape and the loading of the metal on the inorganic matrix may also be of great importance [28–33]. Here, we report of the extension of the MVS technique to the preparation of supported gold nanoparticles with different sizes and metal loadings, and of a detailed investigation of the factors that can affect their catalytic activity in the hydrosilylation of 1-hexyne with Et_3SiH, this being chosen as the reference reaction.

2. Experimental

2.1. General

All operations involving the products from Metal Vapour Synthesis (MVS) were performed under a dry argon atmosphere. The co-vaporization of gold and acetone was carried out in a static reactor as previously described [34]. The "acetone-solvated Au atoms" solution was worked up under argon atmosphere with the use of standard Schlenk techniques. The amount of gold in these solutions was determined by atomic absorption spectrometry in an electrically heated graphite furnace with a Perkin–Elmer 4100ZL instrument. Acetone was purified by conventional methods, distilled and stored under argon. 1-Hexyne and triethylsilane were commercial products, and were distilled and degassed before use. Commercial γ-Al_2O_3 (Chimet product, type 49, 3.1 μm average particle size, surface area 110 $m^2\,g^{-1}$), C (Chimet product, surface area 890 $m^2\,g^{-1}$), TiO_2 (Aldrich product, powder, ⩾99.9%, 1.0 μm average particle size, surface area 5.8 $m^2\,g^{-1}$), ZrO_2 (Aldrich product, powder, 99%, 0.88 μm average particle size, surface area 4.9 $m^2\,g^{-1}$), Fe_2O_3 (Aldrich product, powder, 99.5%, 1.0 μm average particle size, surface area 2.1 $m^2\,g^{-1}$), CeO_2 (Aldrich product, powder, ⩾99.9%, 1.45 μm average particle size, surface area 2.0 $m^2\,g^{-1}$) were dried in a static oven before use. The GLC analyses were performed on a Perkin–Elmer Auto System gas chromatograph, equipped with a flame ionization detector (FID), using a SiO_2 column (DB1, 30 m × 0.52 mm, 5 μm) and helium as carrier gas.

2.2. Preparation of catalysts

In a typical experiment, gold vapours generated by resistive heating of an alumina crucible filled with ca. 500 mg of gold pellets were co-condensed at liquid nitrogen temperature with acetone (100 ml) in the glass reactor chamber of the MVS apparatus for a chosen time. The reactor chamber was warmed to the melting point of the solid matrix, and the resulting deep purple solution was siphoned at a low temperature into a Schlenk tube and kept in a refrigerator at −20 °C. Three different gold/acetone "solutions" were prepared in which 0.16, 0.43 and 1.42 mg Au/ml acetone were present as determined by atomic absorption analysis. Pairs of catalysts with the same final Au content were prepared from different amounts of gold/acetone solutions with low (0.16 mg Au/ml acetone) or high (1.42 mg Au/ml acetone) gold concentration. The member of such pairs will be labelled as LC or HC, respectively.

2.2.1. Preparation of Al_2O_3-supported catalysts

Au/γ-Al_2O_3 (0.05%, w/w). 1.6 ml (0.25 mg Au) of the gold/acetone solution (0.16 mg/ml) were added to a suspension of 0.5 g of γ-Al_2O_3 in acetone (20 ml). The mixture was stirred for 2 h at room temperature and the colourless supernatant solution was removed with a siphon. The solid was washed with 20 × 2 ml of *n*-pentane, and dried under reduced pressure.

Au/γ-Al_2O_3 (0.10%, w/w, LC). 15 ml (2.4 mg Au) of the gold/acetone solution (0.16 mg/ml) were added to a suspension of 2.4 g of γ-Al_2O_3 in acetone (20 ml). The mixture was stirred for 2 h at room temperature, and the colourless supernatant solution was removed with a siphon. The solid was washed with 20 × 2 ml of *n*-pentane and dried under reduced pressure.

Au/γ-Al_2O_3 (0.10%, w/w, HC). 1.4 ml (2 mg Au) of the gold/acetone solution (1.42 mg/ml) were added to a suspension of 2 g of γ-Al_2O_3 in acetone (30 ml). The mixture was stirred for 24 h at room temperature, and the colourless supernatant solution was removed with a siphon. The solid was washed with 20 × 2 ml of *n*-pentane and dried under reduced pressure.

Au/γ-Al_2O_3 (0.50%, w/w). 11.6 ml (5 mg Au) of the gold/acetone solution (0.43 mg/ml) were added to a suspension of 1 g of γ-Al_2O_3 in acetone (20 ml). The mixture was stirred for 24 h at room temperature, and the colourless supernatant solution was removed with a siphon. The solid was washed with 20 × 2 ml of *n*-pentane and dried under reduced pressure.

Au/γ-Al_2O_3 (2.00%, w/w). 9.3 ml (4 mg Au) of the gold/acetone solution (0.43 mg/ml) were added to a suspension of 0.2 g of γ-Al_2O_3 in acetone (10 ml). The mixture was stirred for 24 h at room temperature, and the colourless supernatant solution was removed with a siphon. The solid was washed with 20 × 2 ml of *n*-pentane and dried under reduced pressure.

2.2.2. Preparation of carbon-supported catalysts

Au/C (0.10%, w/w, LC). 15 ml (2.4 mg Au) of the gold/acetone solution (0.16 mg/ml) were added to a suspension of 2.4 g of carbon in acetone (20 ml). The mixture was stirred for 48 h at room temperature. The organic phase was removed under vacuum and the solid was dried (0.1 mmHg).

Au/C (0.10%, w/w, HC). 1.4 ml (2 mg Au) of the gold/acetone solution (1.42 mg/ml) were added to a suspension of 2 g of carbon in acetone (30 ml). The mixture was stirred for 48 h at room temperature. The organic phase was removed under vacuum and the solid was dried (0.1 mmHg).

2.2.3. Preparation of MeO_x-supported catalysts

Au/Fe_2O_3 (0.10%, w/w). 2.4 ml (1 mg Au) of the gold/acetone solution (0.43 mg/ml) were added to a suspension of 1 g of Fe_2O_3 in acetone (20 ml). The mixture was stirred for 24 h at room temperature. The colourless supernatant solution was removed with a siphon, and the solid was washed with 20 × 2 ml of *n*-pentane and dried under reduced pressure.

Au/Fe_2O_3 (4.50%, w/w). 21 ml (9 mg Au) of the gold/acetone solution (0.43 mg/ml) were added to a suspension of 0.2 g of Fe_2O_3 in acetone (10 ml). The mixture was stirred for 24 h at room temperature. The organic layer was removed under vacuum and the solid was dried (0.1 mmHg).

Au/TiO_2 (0.10%, w/w). 2.4 ml (1 mg Au) of the gold/acetone solution (0.43 mg/ml) were added to a suspension of 1 g of TiO_2 in acetone (20 ml). The mixture was stirred for 48 h at room temperature. The organic layer was removed under vacuum and the solid was dried (0.1 mmHg).

Au/TiO_2 (1.48%, w/w). 3.4 ml (1 mg Au) of the gold/acetone solution (0.43 mg/ml) were added to a suspension of 1 g of TiO_2 in acetone

(20 ml). The mixture was stirred for 48 h at room temperature. The organic layer was removed under vacuum and the solid was dried (0.1 mmHg).

Au/CeO_2 (0.10%, w/w). 2.4 ml (1 mg Au) of the gold/acetone solution (0.43 mg/ml) were added to a suspension of 1 g of CeO_2 in acetone (20 ml). The mixture was stirred for 48 h at room temperature. The organic phase was removed under vacuum and the solid was dried (0.1 mmHg).

Au/ZrO_2 (0.10%, w/w). 2.4 ml (1 mg Au) of the gold/acetone solution (0.43 mg/ml) were added to a suspension of 1 g of ZrO_2 in acetone (20 ml). The mixture was stirred for 48 h at room temperature. The organic layer was removed under vacuum and the solid was dried (0.1 mmHg).

2.3. Catalytic tests

Catalytic runs were carried out in Pyrex Carius tubes fitted with Rotaflo taps. To a certain amount of Au/support were added via syringe 4 mmol (0.46 ml) of 1-hexyne and 2 mmol of the triethylsilane (0.16 ml). The suspension was stirred for a chosen time at the reported temperature and filtered on Celite, and the filtrate was evaporated under vacuum to remove the excess 1-hexyne. The crude products were characterized by GC analysis and their ^{1}H NMR proton signals.

2.4. Characterization of the catalysts

Electron micrographs were obtained with a Jeol 2000EX microscope. Before being introduced into the instrument, the samples, in the form of powders, were ultrasonically dispersed in isopropyl alcohol and a drop of the suspension was deposited on a copper grid covered with a lacy carbon film. Mean particle sizes (d_m) were calculated from the formula $d_m = \sum d_i n_i / \sum n_i$, where n_i is the number of particles of diameter d_i, while the width of the distribution was evaluated from its standard deviation, $\sigma = (\sum d_i - d_m)^2 \big/ (\sum n_i)^{0.5}$. The metal surface area (MSA) of the gold particles (by assuming a hemispherical shape) was calculated by the formula: $\mathrm{MSA} = 3\sum n_i r_i^2 / 2\rho_{Au} \sum n_i r_i^3$, where r_i is the mean radius of the size class containing n_i particles, and ρ_{Au} is the volumetric mass of Au (19.31 g/cm^3).

3. Results and discussion

Initially we focused our attention on the preparation of various catalysts based on the Metal Vapour Synthesis (MVS) technique; several samples of gold nanoparticles dispersed on inorganic supports, such as γ-Al_2O_3, carbon, Fe_2O_3, TiO_2, CeO_2 and ZrO_2, and with different metal loadings were obtained.

3.1. Preparation and characterization of the catalysts

Gold nanoparticles were prepared by means of the MVS technique. According to previously described procedures [33], gold and acetone were vaporized under vacuum and deposited on the frozen walls (−198 °C) of a glass reactor, generating a purple solid matrix. During the warm-up stage from −196 to −20 °C the matrix melted, and nucleation and growth processes of the metal particles took place leading to gold nanoclusters weakly stabilized by the acetone molecules, the so-called "solvated metal atoms". These MVS "solutions" of Au/CH_3COCH_3 were then added at room temperature to a suitable amount of the support till decolourization of the suspension occurred, which is indicative of the complete deposition of the Au particles on the inorganic matrices.

Motivated by the extensive work of Klabunde and co-workers [34,35] on the influence of the gold content in the solutions of acetone-solvated atoms on the sizes of the nanoparticles in the resulting powders, we prepared Au/CH_3COCH_3 co-condensates with different gold/acetone concentrations: 0.16 mg/ml (low concentration, LC) and 1.42 mg/ml (high concentration, HC), respectively. These systems were used as the starting materials for the deposition of Au nanoparticles on supports as depicted in Scheme 1.

The morphological features of these catalytic systems were investigated by HRTEM. The micrographs and the size distributions of the metal particles obtained for Au/C and Au/γ-Al_2O_3 prepared from LC and HC solutions are displayed in Fig. 1.

It can be observed that gold nanoparticles deposited on both supports from LC solutions exhibit a very similar particle size distribution over the 2.0–10.0 nm range, with an average diameter ($\langle d \rangle$) of ca. 4.8 nm and a width (σ) of ca. 2.00 nm (Fig. 1 a and b). In contrast, the catalysts prepared from HC solutions exhibit a notably wider distribution of metal particle size (4.0–20 nm), with a significant fraction of particles larger than 10 nm in size (Fig. 1 c and d). Furthermore, the large particles appeared to be polycrystalline in nature, as shown in the inset of Fig. 1d. In agreement with Klabunde's observations [35], our results indicate the important influence exerted by the concentration of the MVS solution on the aggregation phenomena of the nanoparticles and consequently on their dimensions.

Next, starting from MVS diluted "solutions" of Au/CH_3COCH_3 (0.16–0.43 mg/ml) we prepared three samples of nanoparticles supported on alumina characterized by different metal loading (0.05%, 0.50% and 2.00%, w/w). We were particularly intrigued by the possibility of keeping the particle sizes very small even when the amount of metal on the support was increased. The corresponding HRTEM histograms are displayed in Fig. 2.

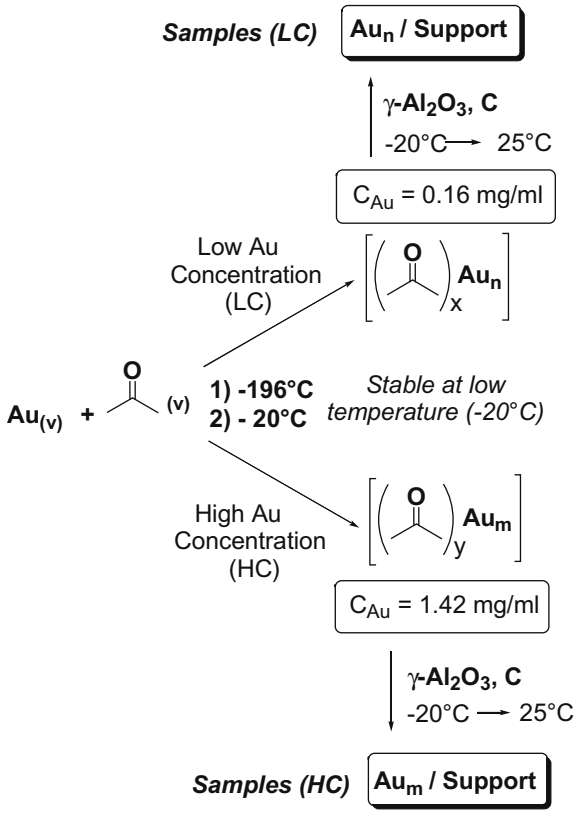

Scheme 1. Preparation of high concentration (HC) and low concentration (LC) supported gold nanoparticles.

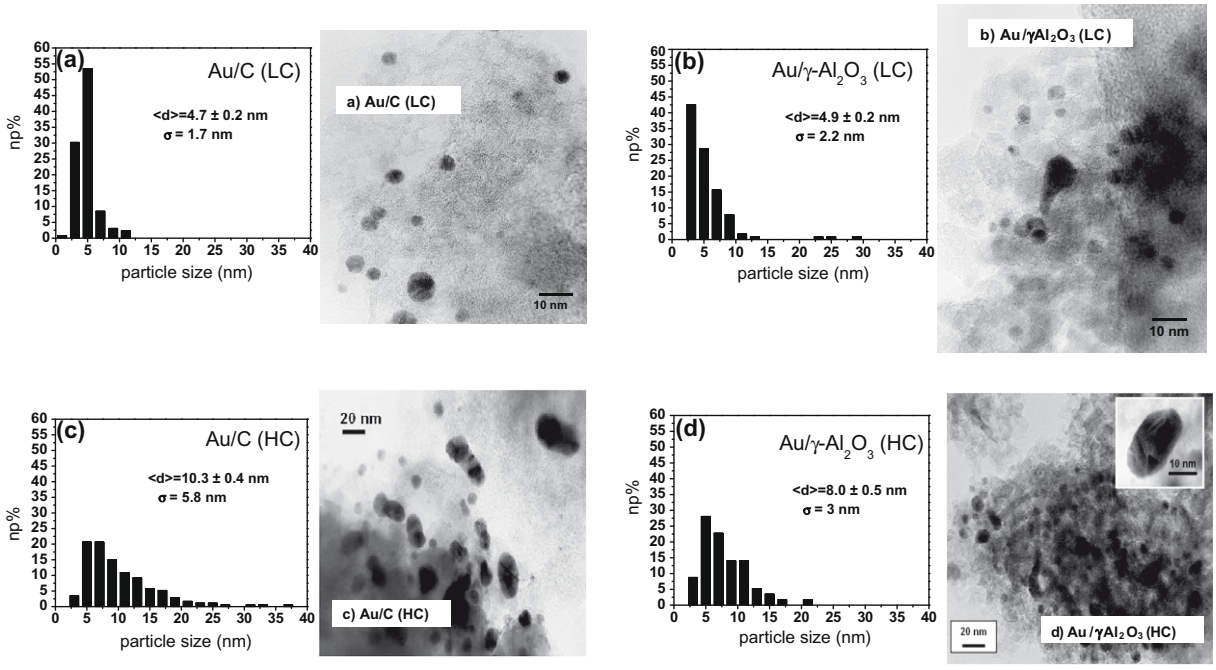

Fig. 1. HRTEM micrographs and gold particle size distributions of supported gold nanoparticles, 0.10 wt%, on γ-alumina and carbon starting from a concentration of 0.16 mg/ml (LC) and 1.42 mg/ml (HC), respectively.

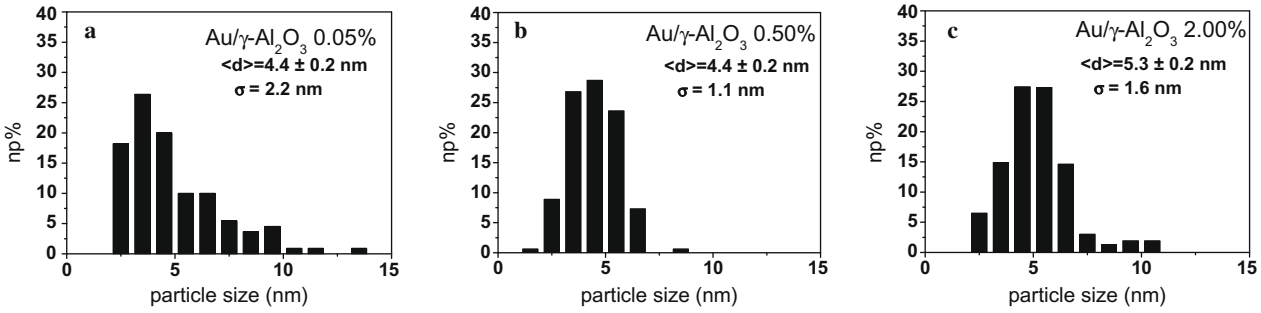

Fig. 2. HRTEM histograms of gold particle size distributions of $Au/\gamma\text{-}Al_2O_3$ 0.05% (a), 0.50% (b) and 2.00% (c) (w/w).

Analogously to the results of the HRTEM analysis on the LC samples (Fig. 1), the histograms of the size distribution of metal particles of the three catalysts appeared quite narrow (2–12 nm) with the mean diameter slightly increasing from 4.4 to 5.3 nm, when the metal loading was increased from 0.05% to 2.00% (w/w) (Fig. 2). It can be noticed that the histograms related to the catalysts with the lower Au loading (0.05 wt%, Fig. 2a; 0.10 wt%, Fig. 1b) exhibited the larger standard deviation because of the broadening towards sizes larger than 5 nm. As it is quite unexpected that larger relative amounts of bigger particles are formed at lower metal loading, this feature suggests that the 0.05 wt% Au and 0.10 wt% Au catalysts should contain a number of very small Au particles (then likely belonging to the class of clusters), more abundant for 0.05 wt% Au, that escaped the detection by HRTEM.

Nevertheless, the microscopy analysis results confirmed that nanoparticles essentially smaller than 10 nm in size and homogeneously dispersed on $\gamma\text{-}Al_2O_3$ can be generated if diluted solutions of gold/acetone were chosen as starting material.

Finally, using the 0.43 mg/ml Au/CH_3COCH_3 co-condensate, we prepared four gold species deposited on CeO_2, Fe_2O_3, TiO_2 and ZrO_2 with a metal loading of 0.10% (w/w) in order to investigate the possible effects of the different supports on the Au nanoparticles size. Representative HRTEM images and particle size distributions are reported in Fig. 3.

In general, the dispersion of Au on the support appeared highly homogeneous for all the samples considered, and the size of the particles lay mostly between 2.0 and 8.0 nm. The resulting size distributions exhibited some common features along the series of the four materials: quite narrow (between 1.5 and 2.1 nm) around the mean value, which lay in the 3.7–4.9 nm range, and slightly asymmetric towards the larger sizes, especially for the Au/TiO_2 system. In this last case, general, HRTEM micrographs revealed a hemispheric/polyhedral shape for the gold nanoparticles deposited on the metal oxides, with a quite wide area of interaction with the support (see inset in Fig. 3).

These results clearly demonstrated that the dimensions of the gold nanoparticles depended strictly on the metal concentration of the co-condensate precursors, but were only slightly affected by the nature of the inorganic matrices chosen for the preparation of the supported catalysts.

This trend was confirmed by the gold particle size distributions of two catalysts, Au/Fe_2O_3 (4.50%), and Au/TiO_2 (1.48%), obtained by the deposition of a diluted MVS solution (0.43 mg/ml) (Fig. 4).

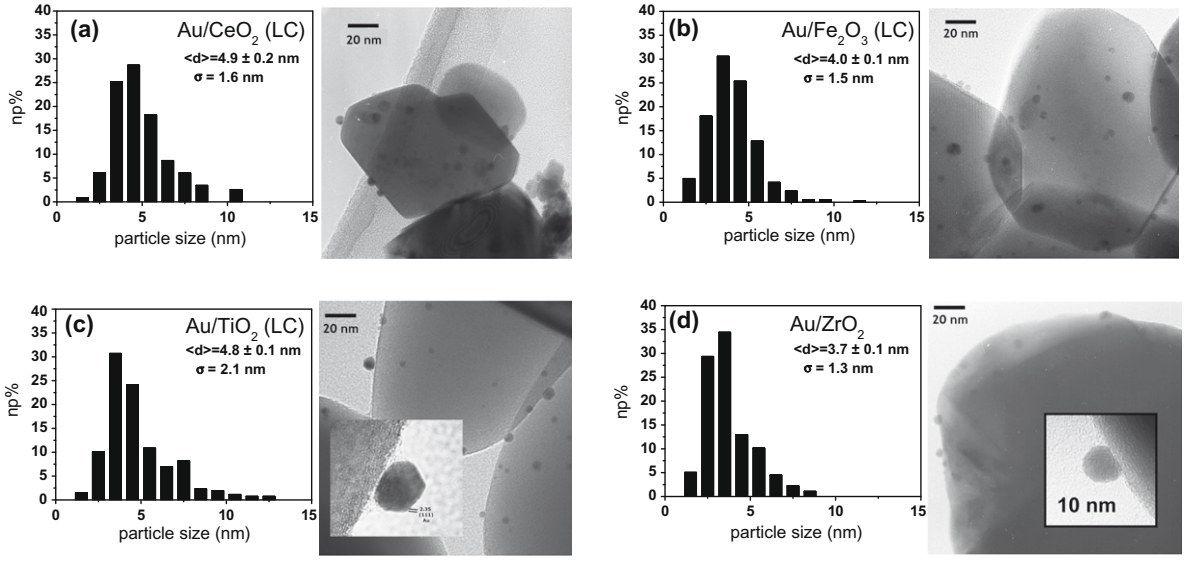

Fig. 3. HRTEM micrographs and gold particle size distributions of supported gold nanoparticles, 0.10% (w/w), on CeO_2 (a), Fe_2O_3 (b), TiO_2 (c) and ZrO_2 (d) prepared from gold/acetone concentration of 0.43 mg/ml (LC). Insets: Details showing the particle-support interaction.

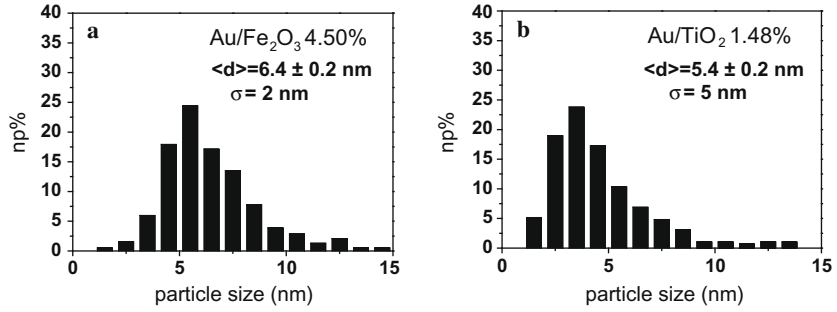

Fig. 4. HRTEM histograms of Au/Fe_2O_3 (4.50%, w/w) (a) and Au/TiO_2 (1.48%, w/w) (b) obtained from Au/CH_3COCH_3 0.43 mg/ml solution.

As already observed for the alumina-supported gold nanoparticles (Fig. 2), a large increase of the metal loading from 0.10% to 4.50% or 1.48% (w/w) did not cause much variation of the gold particles sizes, which were now in the range of 5.4–6.4 nm with respect to 4.0–4.8 nm (Fig. 3b and c vs. Fig. 4a and b, respectively).

3.2. Hydrosilylation reactions

The catalytic activity of the prepared catalysts was then evaluated in the hydrosilylation of 1-hexyne with Et_3SiH; the reactions were performed without solvent, at 90 °C, with a molar ratio substrate/Au = 2000 mmol/mmol (Scheme 2). First of all, the performances of the supported gold nanoparticles prepared form the LC and HC solutions (Fig. 1) were evaluated. The obtained results are summarized in Table 1.

As highlighted by the reported data, the $Au/\gamma\text{-}Al_2O_3$ (LC) and Au/C (LC) (0.1%, w/w) catalysts showed very high activity (Table 1, SA = 6480, entry 1, and 5680, entry 2, respectively) and regioselectivity towards the (**E**)-**3** isomer (Table 1, 93% and 98%, entries 1 and 2). By contrast, the analogous $Au/\gamma\text{-}Al_2O_3$ (HC) and Au/C (HC) systems prepared from more concentrated gold/acetone solutions (1.42 mg/ml), and containing particles of larger diameter (4–20 nm, Fig. 1), were completely inactive even after long reaction times. These results confirmed a good correlation between the nanoparticles sizes and the catalytic activity of gold as already observed by Haruta in his pioneer work on CO oxidation [1].

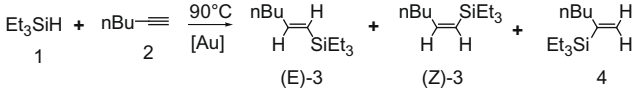

Scheme 2. Hydrosilylation of 1-hexyne with Et_3SiH catalyzed by supported gold nanoparticles.

Intrigued by these initial data, we tested in the hydrosilylation process of 1-hexyne with Et_3SiH the $Au/\gamma\text{-}Al_2O_3$ catalysts characterized by different metal loadings (0.05%, 0.50% and 2.00%, w/w, Fig. 2) and obtained starting from diluted MVS solutions (0.16–0.43 mg/ml) (Table 2).

All the employed catalysts were very active and selective towards the formation of (E)-1-(trimethylsilyl)-1-hexene (**E**)-**3**, although a reduction of the catalytic efficiency was observed when the gold amount on the support increased. Indeed, the lower was the metal loading, the higher was the specific activity (Table 2, entry 1). Considering that the HRTEM analysis had shown similar nanoparticle dimensions for the four catalysts (Figs. 1b and 2), the catalytic performance of the 0.05% $Au/\gamma\text{-}Al_2O_3$ sample could be ascribed to the presence of very small nanocluster that might escape the detection by TEM. Another fact that could influence the specific activity of the 0.05% $Au/\gamma\text{-}Al_2O_3$ sample could be the high dispersion of the gold on alumina and consequently the presence of isolated Au nanoparticles readily available for the catalysis.

At this stage, our investigation was devoted to the catalytic activity of the nanoparticles deposited on different supports

Table 1
Hydrosilylation of 1-hexyne promoted by LC and HC Au/C and Au/γ-Al_2O_3 (0.1%, w/w).[a]

Entry	Catalyst (0.1%, w/w)	*t*	Conv. (%)[b]	Selectivity (%)[b]			Specific activity, SA (h^{-1})[c]
				(**E**)-**3**	(**Z**)-**3**	**4**	
1	Au/γ-Al_2O_3 (LC)	15 min	81	93	3	4	6480
2	Au/C (LC)	15 min	71	98	0	2	5680
3[d]	Au/γ-Al_2O_3 (HC)	1 h	0	–	–	–	0
4[d]	Au/C (HC)	1 h	0	–	–	–	0

[a] Reaction conditions: 4 mmol of 1-hexyne, 1 mmol of Et_3SiH, 5×10^{-4} mmol of Au, 90 °C.
[b] Obtained by GC and ^1H NMR analysis.
[c] Specific activity is calculated as mmol of products/(mmol of gold × h).
[d] Catalysts obtained starting from concentrated Au/acetone solution (1.42 mg Au/ml).

Table 2
Hydrosilylation of 1-hexyne promoted by Au/γ-Al_2O_3 with different metal loadings.[a]

Entry	Metal loading (%, w/w)	*t* (min)	Conv. (%)[b]	Selectivity (%)[b]			Specific activity, SA (h^{-1})[c]
				(**E**)-**3**	(**Z**)-**3**	**4**	
1[d]	0.05	15	59	97	–	3	9440
2	0.10	15	81	98	0	2	6480
3	0.50	30	83	94	2	4	3320
4	2.00	30	75	91	4	5	3000

[a] Reaction conditions: 4 mmol of 1-hexyne, 1 mmol of Et_3SiH, 5×10^{-4} mmol of Au, 90 °C.
[b] Obtained by GC and ^1H NMR analysis.
[c] Specific activity is calculated as mmol of products/(mmol of gold × h).
[d] Reaction performed with 2.5×10^{-4} mmol of Au.

(CeO_2, Fe_2O_3, TiO_2 and ZrO_2 characterized by similar superficial areas, i.e., 2–6 $m^2\ g^{-1}$, and chemical purity >99%) but with the same amount of gold (0.1%, w/w) prepared from the 0.43 mg/ml solution of Au/CH_3COCH_3. These samples were studied in the hydrosilylation reaction (Scheme 2 and Table 3) under the same reaction conditions as for the previously reported Au/γ-Al_2O_3 and Au/C systems (Table 1).

As can be seen from Table 3, the MVS-derived gold nanoparticles, prepared from solvated Au atoms at low concentration, deposited on ceria (Table 3, entry 1) and iron oxide (Table 3, entry 2) showed high catalytic activity, which was comparable with those previously reported for Au/γ-Al_2O_3 (LC) (Table 1, entry 1) and Au/C (LC) (Table 1, entry 2) species. In particular, the Au/CeO_2 catalyst showed the best efficiency leading to the E isomer with a specific activity of 6480 h^{-1} and a selectivity of 98%. In contrast, Au/TiO_2 and Au/ZrO_2 samples showed high selectivity towards (**E**)-**3** (Table 3, entries 3 and 4, 95% and 96%, respectively), but displayed significantly lower specific activities (3840 and 1600 h^{-1}) than the other tested catalysts.

The morphological features of the four catalysts obtained from the HRTEM analysis (Fig. 3) were not sufficient to rationalize the different behaviour observed. Indeed, all the supported gold nanoclusters had diameters between 2 and 8 nm, and resulted highly dispersed on the inorganic matrices. Nevertheless, the shape of the distributions and the relative population of the classes exhibited some differences. The metal specific surface area (SSA) was therefore calculated (as indicated in Section 2), resulting in the following values: 25, 28, 20 and 32 $m^2\ g^{-1}$, for the Au/CeO_2, Au/Fe_2O_3, Au/TiO_2 and Au/ZrO_2 catalysts, in the order (Table 3, column 8). However, the differences among these values could not account for the different catalytic behaviour of the materials, as can be inferred from the observed trends of the relative specific activity and relative specific metal surface areas (Table 3, columns 7 and 9).

Furthermore, differences in the relative abundance of the various size classes cannot easily account for the differences in catalytic activity. For instance, in the case of the most active catalyst (Au/CeO_2, Fig. 3a), ca. 70% of the Au particles are larger than 4 nm, while particles of this size account only for 30% of the metal phase present in the Au/ZrO_2 catalyst (Fig. 3d), the less active one, but this correlation does not hold for the other two systems.

Thus, other features of the metal particles should also contribute to the activity in the title reactions, such as particular surface geometric and electronic states resulting from a proper combination of size, shape and interaction with the support. As for this last aspect, during TEM observation of Au/TiO_2 and Au/ZrO_2, few Au particles appeared suitably located on the surface of the grains of the supports to allow the observation of an extended interface with the support (see insets of Fig. 3c and d). Unluckily, no metal particles properly oriented to obtain equivalent images were observed in the case of Au/CeO_2 and Au/Fe_2O_3.

Table 3
Hydrosilylation of 1-hexyne with Et_3SiH performed with Au nanoparticles deposited on different supports.[a]

Entry	Catalyst (0.1%, w/w)	Selectivity (%)[b]			Specific activity (SA) (h^{-1})[c]	Relative specific activity	Estimated metal specific surface area ($m^2\ g^{-1}$)[d]	Relative metal specific surface area
		(**E**)-**3**	(**Z**)-**3**	**4**				
1	Au/CeO_2	98	0	2	6480	1	25	1
2	Au/Fe_2O_3	92	0	8	6160	0.95	28	1.12
3	Au/TiO_2	95	2	3	3840	0.59	20	0.80
4	Au/ZrO_2	96	0	4	1600	0.25	32	1.28

[a] Reaction conditions: 4 mmol of 1-hexyne, 1 mmol of Et_3SiH, 5×10^{-4} mmol of Au, 90 °C, 15 min.
[b] Obtained by GC and ^1H NMR analysis.
[c] Specific activity is calculated as mmol of products/(mmol of gold × h).
[d] Calculated as described in Section 2.

Table 4
Specific activities and selectivity for commercial and MVS supported catalysts.[a]

Entry	Catalyst	Metal loading (%, w/w)	*t* (min)	Conv. (%)[b]	Selectivity (%)[b]			Specific activity, SA (h^{-1})[c]
					(**E**)-**3**	(**Z**)-**3**	**4**	
1	$Au/Fe_2O_{3(COM)}$	4.50	30	60	95	–	5	2400
2	$Au/Fe_2O_{3(MVS)}$	4.50	30	85	95	1	4	3420
3	$Au/Fe_2O_{3(MVS)}$	0.10	15	77	92	0	8	6160
4	$Au/TiO_{2(COM)}$	1.48	15	90	99	–	1	7200
5	$Au/TiO_{2(MVS)}$	1.48	15	83	98	–	2	6640
6	$Au/TiO_{2(MVS)}$	0.10	15	48	95	2	3	3840

[a] Reaction conditions: 4 mmol of 1-hexyne, 1 mmol of Et_3SiH, 5×10^{-4} mmol of Au, 90 °C.
[b] Obtained by GC and ^1H NMR analysis.
[c] Specific activity is calculated as mmol of products/(mmol of gold × h).

In order to examine the catalytic potential of the Metal Vapour Synthesis technique, the performances of the MVS supported nanoparticles were then compared with those of commercially available species. Indeed, some years ago, the World Gold Council began to purchase gold nanoparticles with a mean diameter of 3.7–3.8 nm, deposited on Fe_2O_3 and TiO_2 with metal loadings of 4.50% and 1.48% (w/w), respectively. As a consequence, using the diluted 0.43 mg/ml solution of gold/acetone, we prepared two samples of Au/Fe_2O_3 (4.50%) and Au/TiO_2 (1.48%) which were tested in the reference reaction together with the commercial catalysts (Scheme 2 and Table 4).

As is clear from the reported data, the commercial and the MVS catalysts with the same amount of supported metal showed similar selectivity and reaction rates (Table 4, entries 1, 2, 4 and 5). It is noteworthy that HRTEM analysis of the gold nanoparticles coming from the MVS solutions (Fig. 4) had showed larger sizes (5.4–6.4 nm) than the commercial ones (3.7–3.8 nm), thus indicating a greater efficiency of the active sites of the MVS nanoparticles.

Moreover, as already detected in the reactions promoted by Au/γ-Al_2O_3 (Table 2, entries 2 and 4), when the hydrosilylation process was performed in the presence of gold nanoparticles supported on Fe_2O_3 with a 4.50% (w/w) metal loading, the value of the specific activity was about half of that of the 0.10% (w/w) sample (Table 4, entry 2 vs. entry 3). This result can be explained once more with a greater dispersion of the metal observed for the 0.1% (w/w) Au/Fe_2O_3 catalyst (Fig. 3b).

On the contrary, in the case of Au/TiO_2 species, the sample with larger quantities of gold (1.48%, w/w) was much more reactive than the corresponding 0.10% (w/w) catalyst. The changes in the metal particle size distribution of the two samples cannot account for the increase of specific activity as the Au/TiO_2 with the higher loading exhibits larger mean particle size and a broader distribution. It is worth noticing, however, that a larger fraction of small particles (below 3 nm) are observed in the 1.48% (w/w) Au/TiO_2 catalyst. Since it is quite unlikely that smaller particles are produced by increasing the metal loading, it can be hypothesized that in the 0.10% (w/w) Au/TiO_2 a significant part of gold is present in the form of very small particles/clusters (below 1 nm, not observable by TEM) [36]. Under this hypothesis, the poorer catalytic performance of the 0.10 wt% Au/TiO_2 suggests a lower activity of such small particles/clusters, on the contrary of what was proposed in the case of Au/Al_2O_3. Such an opposite behaviour might be the consequence of a different metal/support interaction (“interface effect”) [37], particularly important in the case of very small particles.

4. Conclusion

In conclusion, we have found that solvated gold atoms prepared according to the Metal Vapour Synthesis technique can be used for the preparation of supported species that provide active catalysts for the hydrosilylation of terminal acetylenes with high regioselectivity (>90%) for the E isomer. Two main factors seem to play an important role in the catalytic performance of the supported species: the size of the gold particles and their interaction with the support. As clearly indicated by the HRTEM analysis, diluted MVS solutions give rise to highly dispersed small gold particles that show very good specific activity, whereas concentrated solvated metal atoms generate supported nanoclusters with a larger size distribution and mean diameter, which are totally inactive. On the other hand, starting from a diluted Au/CH_3COCH_3 co-condensate, supported catalysts with different metal loadings on the matrices can be prepared without loss of reactivity. Indeed, the increase of the metal content on the support (0.05–4.50%, w/w) does not cause a marked growth of the gold nanoparticles, the mean diameter lying in the range between 4.0 and 5.8 nm. However, ZrO_2- and TiO_2-supported catalysts did not follow this general trend. In these cases, a strong interfacial contact between Au and the metal oxide could reduce the number of active sites of the catalysts; an increase of the gold amount on the support then improves the catalytic efficiency of these species.

Acknowledgment

L.B. and G.M. acknowledge the Compagnia di San Paolo for the financial support to the NIS.

References

[1] M. Haruta, T. Kobayashi, H. Sano, N. Yamada, Chem. Lett. (1987) 405.
[2] G.J. Hutchings, J. Catal. 96 (1985) 292.
[3] G.J. Hutchings, M. Brust, H. Schibaur, Chem. Soc. Rev. 37 (2008) 1759.
[4] R. Skouta, C. Li, Tetrahedron 64 (2008) 4917.
[5] A. Corma, H. Garcia, Chem. Soc. Rev. 37 (2008) 2096.
[6] J.C. Fierro-Gonzalez, B.C. Gates, Chem. Soc. Rev. 37 (2008) 2127.
[7] M. Chen, D.W. Goodman, Chem. Soc. Rev. 37 (2008) 1860.
[8] A.S.K. Hashmi, Chem. Rev. 107 (2007) 3180.
[9] A.S.K. Hashmi, G.J. Hutchings, Angew. Chem., Int. Ed. 45 (2006) 7896.
[10] P. Landon, P.J. Collier, A.J. Papworth, C.J. Kiely, G.J. Hutchings, Chem. Commun. (2002) 2058.
[11] A. Corma, P. Serna, Science 313 (2006) 332.
[12] C. Della Pina, E. Falletta, L. Prati, M. Rossi, Chem. Soc. Rev. 37 (2008) 2077.
[13] G.J. Hutchings, Dalton Trans. (2008) 5523.
[14] A. Abad, A. Corma, H. Garcia, Chem. Eur. J. 14 (2008) 212.
[15] M. Haruta, M. Daté, Appl. Catal. A: Gen. 222 (2001) 427.
[16] J.H. Teles, S. Brode, M. Chabanas, Angew. Chem., Int. Ed. 37 (1998) 1415.
[17] E. Mizushima, K. Sato, T. Hayashi, M. Tanaka, Angew. Chem., Int. Ed. 41 (2002) 4563.
[18] T.E. Muller, M. Beller, Chem. Rev. 98 (1998) 675.
[19] H. Ito, T. Yajima, J. Tateiwa, A. Hosomi, Chem. Commun. (2000) 981.
[20] N. Debono, M. Iglesias, F. Sanchez, Adv. Synth. Catal. 349 (2007).
[21] A. Corma, C. Gonzales-Arellano, M. Iglesias, F. Sanchez, Angew. Chem., Int. Ed. 46 (2007) 7820.
[22] D. Lantos, M. Contel, S. Sanz, A. Bodor, I.T. Horvath, J. Organomet. Chem. 692 (2007) 1799.
[23] B.M. Wile, R. McDonald, M.J. Ferguson, M. Stradiotto, Organometallics 26 (2007) 1069.
[24] D. Lantos, M. Contel, A. Larrea, D. Szabo, I.T. Horvath, QSAR Comb. Sci. 25 (2006) 719.

[25] T. Masaru, F. Hisashi, J. Am. Chem. Soc. 125 (2003) 15742.
[26] A.M. Caporusso, L.A. Aronica, E. Schiavi, G. Martra, G. Vitulli, P. Salvadori, J. Organomet. Chem. 690 (2005) 1063.
[27] K.J. Klabunde, Free Atoms, Cluster and Nanoscale Particles, Academic Press, New York, 1994.
[28] E. Bus, R. Prins, J.A. van Bokhoven, Catal. Commun. 8 (2007) 1397.
[29] M.S. Chen, D.W. Goodman, Catal. Today 111 (2006) 22.
[30] M.P. Casaletto, A. Longo, A.M. Venezia, A. Martorana, A. Prestianni, Appl. Catal. A 302 (2006) 309.
[31] T.V. Choudhary, D.W. Goodman, Appl. Catal. A: Gen. 291 (2005) 32.
[32] C. Mohr, H. Hofmeister, P. Claus, J. Catal. 213 (2003) 86.
[33] G. Vitulli, C. Evangelisti, A.M. Caporusso, P. Pertici, N. Panziera, S. Bertozzi, Salvadori, in: B. Corain, G. Schmid, N. Toshima (Eds.), Metal Nanoclusters in Catalysis Materials Science: The Issue of Size-Control, Elsevier, Amsterdam, 2007 (Chapter 32).
[34] M.T. Franklin, K.J. Klabunde, in: K. Suslick (Ed.), Living Colloidal Metal Particles from Solvated Metal Atoms. Clustering of Metal Atoms in Organic Media, ACS Chemistry Series, vol. 333, 1987, p. 246.
[35] S.T. Lin, M.T. Franklin, K.J. Klabunde, Langmuir 2 (1986) 259.
[36] C. Evangelisti, G. Vitulli, E. Schiavi, M. Vitulli, S. Bertozzi, P. Salvadori, L. Bertinetti, G. Martra, Catal. Lett. 116 (2007) 57.
[37] M. Azar, V. Caps, F. Morfin, J.-L. Rousset, A. Piednoir, J.-C. Bertolini, L. Piccolo, J. Catal. 239 (2006) 307.